



# A cobalt-free composite cathode prepared by a superior method for intermediate temperature solid oxide fuel cells

Zhiwen Zhu<sup>a</sup>, Litao Yan<sup>b</sup>, Wenping Sun<sup>a</sup>, Haowei Liu<sup>a</sup>, Tong Liu<sup>a</sup>, Wei Liu<sup>a,c,\*</sup>

<sup>a</sup> CAS Key Laboratory of Materials for Energy Conversion, Department of Material Science and Engineering, University of Science and Technology of China, Hefei 230026, PR China

<sup>b</sup> Department of Mechanical Engineering, University of South Carolina, Columbia, SC 29208, USA

<sup>c</sup> Key Laboratory of Materials Physics, Institute of Solid State Physics, Chinese Academy of Sciences, Hefei 230031, China

## HIGHLIGHTS

- ▶ SSF–SDC cathode powders were prepared by two different routes.
- ▶ SSF–SDC samples derived from new method showed high electrical conductivity and good catalytic activity.
- ▶ The ASRs of SSF–SDC is comparable to those of other cobalt-free cathode.
- ▶ The SSF–SDC cathode owns good thermal cycle stability.

## ARTICLE INFO

### Article history:

Received 3 February 2012

Received in revised form

23 May 2012

Accepted 12 June 2012

Available online 18 June 2012

### Keywords:

Composite cathode

Symmetrical electrochemical cell

Co-synthesis method

Solid oxide fuel cell

## ABSTRACT

Cobalt-free  $\text{Sm}_{0.6}\text{Sr}_{0.4}\text{FeO}_{3-\delta}-\text{Ce}_{0.8}\text{Sm}_{0.2}\text{O}_{2-\delta}$  (SSF–SDC) composite powders are prepared by a newly one-step synthesis method, co-synthesis method. Powders XRD analysis shows that the composite powders exhibit the consistent phase structure with powders derived from traditional method, which demonstrate that the SSF is compatible with SDC. Dry-mixing method, a traditional composite cathode preparation method, is used to obtain SSF–SDC composite cathode as a comparison. The two cathodic composites of microstructures, electrical conductivities and symmetric electrochemical cells are characterized under the same condition. As a result, powders from new method show superior microstructure, high electrical conductivity and good electrochemical properties. Finally, cathode preparing from new method is evaluated by an anode-supported SDC-electrolyte single cell testing. To further study SSF–SDC cathode, the thermal expansion coefficient and thermal cycling performance are measured. The all results imply that co-synthesis method is a facile and practical way to improve the cathode properties and SSF–SDC is a promising cathode for intermediate temperature SOFCs.

© 2012 Elsevier B.V. All rights reserved.

## 1. Introduction

Solid oxide fuel cells (SOFCs) are thought as electrochemical energy conversion devices which can convert chemical energy into electrical energy with high energy conversion efficiency and low emissions of pollutants [1]. The research of intermediate temperature SOFC has attracted great attention by many groups at last decades, especially for SOFCs based on SDC electrolyte [2–4]. SDC owns high ionic conduction comparing with other ionic conductor below 700 °C. Operation at intermediate temperature will solve

some key issues such as reducing degradation, lessening sealing problems and using cheaper metallic materials as interconnects [5]. However, the low operation temperature of SOFC is negative for the electrochemical processes, e.g., depressing anodic and cathodic reactions, decreasing ion conductivities in electrolyte and resulting in lowering the cell power output. Particularly, cathode process is highly sensitive to temperature due to a high activity energy for oxygen reduction reaction (often >1.5 eV) [6].

A good cathode with low cost and good combination properties need to be found and applied in intermediate temperature SOFCs. Two approaches can be employed to achieve to the required cathode performance. First of all, new material system can be developed for low temperature operation. Cobalt-based cathodes have been extensively studied and show good electrochemical properties, because cobalt-containing cathodes have good catalytic activity for oxygen reduction and high electrical conductivity [7,8].

\* Corresponding author. CAS Key Laboratory of Materials for Energy Conversion, Department of Material Science and Engineering, University of Science and Technology of China, Hefei 230026, PR China. Tel.: +86 551 3602940; fax: +86 551 3601592.

E-mail address: [wliu@ustc.edu.cn](mailto:wliu@ustc.edu.cn) (W. Liu).

However, high thermal expansion coefficient (TEC), poor stability and high cost of cobalt element are encountered for them [9]. Doping ferrite-based cathodes with lower TEC and better stability as well as lower cost are regarded as a development goal [10–12].

In this study, composite cathode  $\text{Sm}_{0.6}\text{Sr}_{0.4}\text{FeO}_{3-\delta}-\text{Ce}_{0.8}\text{Sm}_{0.2}\text{O}_{2-\delta}$  was developed as cathode for intermediate temperature SOFCs. The cathode consists of a perovskite oxide and an oxygen-ion conductor SDC, built in a composite electrode which increases the triple phase boundary (TPB) length and thereby efficiently reduces the electrode polarization and highly improves the thermal compatibility with electrolyte membrane [13,14].

Beside, variety of cathode geometrical parameters can also optimize cathode performance, e.g., porosity [15], particle size [16]. The effect of composite cathode on cell performance can be produced by changing volume fraction and spatial distribution of cathode component [17–19]. SSF–SDC composite cathodes were prepared by two different methods, new co-synthesis method and traditional dry-mixing method. The phase structure, microstructure and electrical properties were contrastively investigated at the same condition. Cathode powders prepared by co-synthesis method showed superior properties.

## 2. Experimental

### 2.1. Powders synthesis

The fine  $\text{Sm}_{0.6}\text{Sr}_{0.4}\text{FeO}_{3-\delta}-\text{Ce}_{0.8}\text{Sm}_{0.2}\text{O}_{2-\delta}$  (SSF–SDC) powders, in which the weight ratio of SSF to SDC was 7:3, were co-synthesized by one-step process using a citrate and nitrate route, namely, co-synthesis method [20]. Required amount of analytical reagents of  $\text{Sm}_2\text{O}_3$ ,  $\text{Sr}(\text{NO}_3)_2$ ,  $\text{Fe}(\text{NO}_3)_3$  and  $\text{Ce}(\text{NO}_3)_3$  were dissolved in dilute nitric acid. Citric acid as complexing agent was added, molar ratio of citric acid/metal equal to 3:2. Then the solution was heated under stirring to evaporate water, changed into viscous gel and finally ignited to flame. The resultant black ash was fired for 3 h at 1000 °C, obtaining SSF–SDC cathode powders.

To compare with new method, dry-mixing method as a traditional preparation method of cathode powders was used to synthesize SSF–SDC powders. SSF and SDC were respectively prepared by the same route as mentioned above, followed by a simple physical mixing them, obtaining the required SSF–SDC composite powders.

### 2.2. Samples preparation

The SSF–SDC powders were shaped into disks with a diameter of 15 mm and bars with 40 mm × 5 mm × 2 mm dimension, uniaxially pressed at 200 Mpa, and sintered at 1400 °C for 10 h. The sintered disks were used to investigate the microstructure. The electrical conductivity measurement was functioned on the sintered bars. Electrical contacts were made using Ag wires and Ag paste placed over whole end faces ensuring a homogeneous current flow.

The SDC powders were pressed into pellets for electrochemical symmetrical cells. The pellets were sintered at 1500 °C for 5 h in air to obtain dense SDC pellets. The cathode slurries (mixing SSF–SDC and 10 wt% ethylcellulose–terpineol binder with the ratio of 1:1) were brush-printed on each side of SDC pellets and then calcined at 1000 °C for 3 h. The half cells, 60 wt% NiO–SDC/SDC bilayers, were prepared by a co-pressing and co-firing process. SSF–SDC cathode slurries were brush-painted on the SDC surface of the half cells, with an area of 0.235 cm<sup>2</sup>, and followed by firing at 1000 °C for 3 h. An anode supported SDC cell with SSF–SDC composite cathode was assembled successfully.

### 2.3. characterizations and testing

The phase composition of powders was identified by an X-ray diffraction (XRD, Philips PW 1730 diffractometer), using Cu K $\alpha$  radiation. A scanning electron microscope (SEM, JSM-6301F) with the mode of backscatter determined the sintered disks microstructure and the cell morphology. The grain size distribution in BSEM images was analyzed using Nano Measurement software. The electrical conductivities were measured in temperature range from 300 to 800 °C at 50 °C intervals using a dc four-probe technique on sintered dense bars. The conductivities ( $\sigma$ ) were determined by taking  $\sigma = L/A \times dI/dV$ , where  $L$  is the distance between voltage contacts and  $A$  is the sample cross section.

Electrochemical symmetrical cells were performed in air from 500 to 700 °C and Ag was used as a current collector for electrode. Polarization resistances ( $R_p$ ) of the cell were measured by an impedance analyzer (CHI604B), applied frequencies range from 0.01 Hz to 100 kHz. Area specific resistances (ASR) were calculated using  $\text{ASR} = R_p \times (\text{surface area})/2$ , where the surface area is 1.187 cm<sup>2</sup>. The thermal cycle tests were performed at temperatures in the range of 200–700 °C. A ramping rate of 5 °C min<sup>−1</sup> was used, followed by a hold at 700 °C for 30 min to measure the polarization resistance during 40 cycles. Electrochemical measurements of a single SOFC were conducted in an Al<sub>2</sub>O<sub>3</sub> test housing placed inside a furnace. Humidified hydrogen (~4% H<sub>2</sub>O) was fed to the anode chamber at a flow rate of 25 mL min<sup>−1</sup>, while the cathode was exposed to atmospheric air. The anode side was sealed with Ag paste. Fuel cell performance was measured with DC Electronic Load (IT8511). Resistances of the cell under open-circuit condition were measured by CHI604B (0.1 Hz–100 kHz). All electrochemical impedance spectra (EIS) were fitted using ZSimpwin software according to LR (QR) equivalent circuit. Thermal expansion of specimen was measured using a dilatometer (SHIMADZU50) at heating rate 10 °C min<sup>−1</sup> in air.

## 3. Results and discussion

### 3.1. Phase composition

Fig. 1 shows XRD patterns of SDC–SSF prepared by two different methods as well as SDC and SSF powders. The peak positions of SSF–SDC from co-synthesis method are consistent with those from dry-mixing method, concluding that SSF–SDC composite cathode

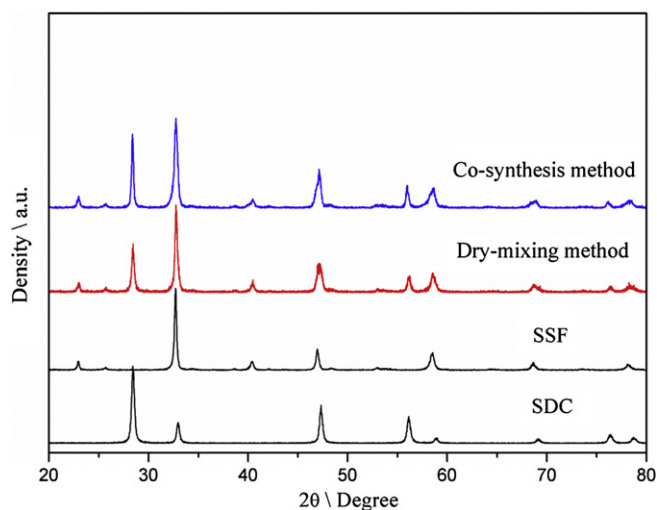


Fig. 1. X-ray powder diffraction patterns of SSF–SDC composite powders derived from co-synthesis and dry-mixing method as well as single SDC and SSF powders.

can be synthesized by new method. It is also easy to find that the composite powders are composed of SSF and SDC, respectively with perovskite and fluorite structure. The XRD patterns reveal that no new phase is formed although there is a difference in solubility of metal ions in the fluorite (SDC) and perovskite (SSF) phases, which indicate that SDC has a good compatibility with SSF after calcining at 1000 °C. The present results are also identical with those reported in reference [21]. The interface reaction and element interdiffusion between cathode and electrolyte will cause performance degeneration [22,23]. From this point of view, SSF–SDC cathode has particular advantage over other cathodes since SSF–SDC powders comes from a co-synthesis process.

### 3.2. Microstructure of sintered samples

Fig. 2 shows the BSEM images of two dense disks (sintered at 1400 °C) at different magnification. The white areas are SDC phase while the dark areas are SSF phase. Comparing between Fig. 2(a) and (b), it is obvious that two phases own a more homogeneous distribution in the disk from co-synthesis method. Previously, Yang et al. [24] investigated the effect of preparation methods on  $\text{Gd}_{0.2}\text{Sr}_{0.8}\text{FeO}_{3-\delta}\text{--}\text{Ce}_{0.8}\text{Gd}_{0.2}\text{O}_{2-\delta}$  membrane microstructures and showed the identified result. In fact, co-synthesis is a chemical mixing method while dry-mixing is a physical mixing method. It can be clarified that chemical mixing is a more effective way for obtaining more homogeneous composite.

The preparation method not only affects homogeneity but also grain sizes of two phases. As shown in Fig. 2(c) and (d), it is also clearly seen that the grain size of the sample from co-synthesis is smaller than that of the sample from dry-mixing. A roughly statistics about grain size was carried out by Nano Measurement soft and showed in Fig. 3(a) and (b). The samples display the mean grain size of SSF and SDC, 0.99  $\mu\text{m}$  and 0.65  $\mu\text{m}$  for co-synthesis method, 1.13  $\mu\text{m}$  and 0.87  $\mu\text{m}$  for dry-mixing method, respectively. Furthermore, SSF and SDC in co-synthesis derived sample exhibit a narrow grain-size distribution than that in dry-mixing

derived sample. In co-synthesis method, SDC and SSF were uniformly scattered in opposing matrix and so inhibit the grain growth of each other, yielding the results as above.

### 3.3. Conductivities measurement

The electrical conductivities of two dense bars were investigated as a function of temperature, shown in Fig. 4(a). In composite, the conductivity of SSF is higher about 2–3 order of magnitude than that of SDC which means two SSF–SDC samples possess a similar conductivity change tendency with characteristics of a small polar conduction. There is a change of growing trend at around 500 °C, which undergoes a semiconducting-like conduction behavior to metal-like conduction behavior. However, due to diversity of microstructure, the sample derived from co-synthesis method has a higher conductivity, 21–56  $\text{S cm}^{-1}$  over the temperature range of 300–800 °C. Since the transport of electrons in perovskite phase is blocked by the fluorite phase in inhomogeneous sample, therefore, the homogeneous sample provides richer electron and oxide ion transport paths and then the corresponding conductivity is higher. The Arrhenius curves of conductivities were plotted in Fig. 4(b). Linear relationships could be observed at low temperature for both samples and the activity energy ( $E_a$ ) was presented according to  $\sigma = C/T \exp(-E_a/kT)$ , where  $k$  is Boltzmann constant and  $C$  is pre-exponential constant. The  $E_a$  is different for both samples, 0.114 eV for co-synthesis and 0.132 eV for dry-mixing over the temperature range of 300–600 °C, respectively. It may be originated from the difference of microstructure. In co-synthesis method, small grain size and uniform two-phase distribution respectively improved the surface activity and charge transportation so as to reduce the corresponding activity energy.

### 3.4. Characterization of symmetrical cells

Fig. 5(a) shows the typical electrochemical impedance spectra (EIS) in Nyquist plot of the SSF–SDC|SDC|SSF–SDC under open-

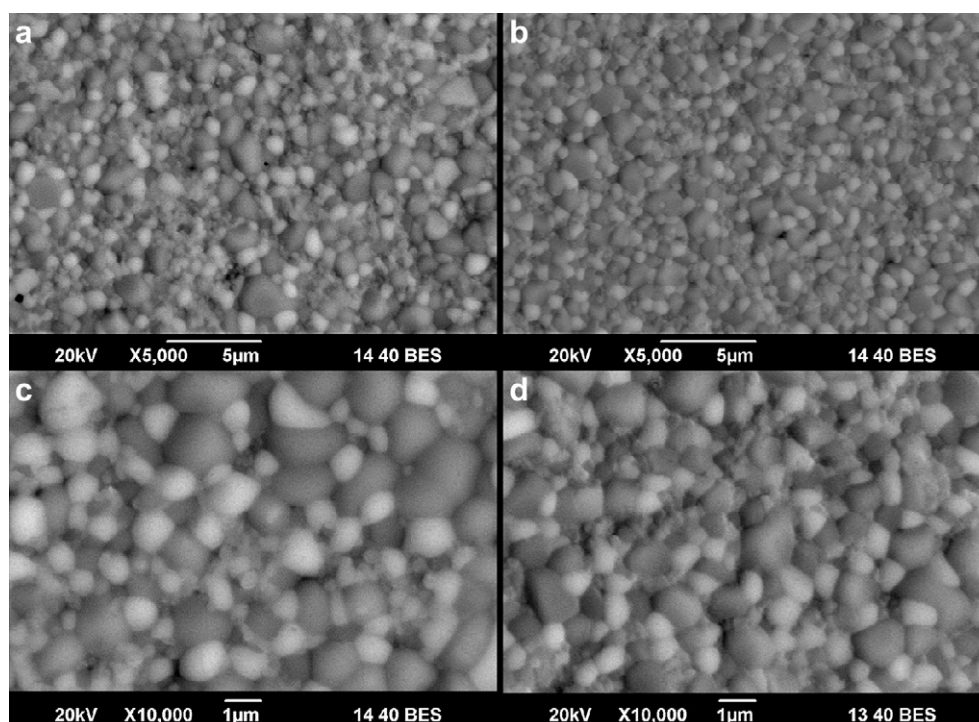


Fig. 2. Backscattered electron images with different magnifications of the thick films from dry-mixing method (a, c) and co-synthesis method (b, d).

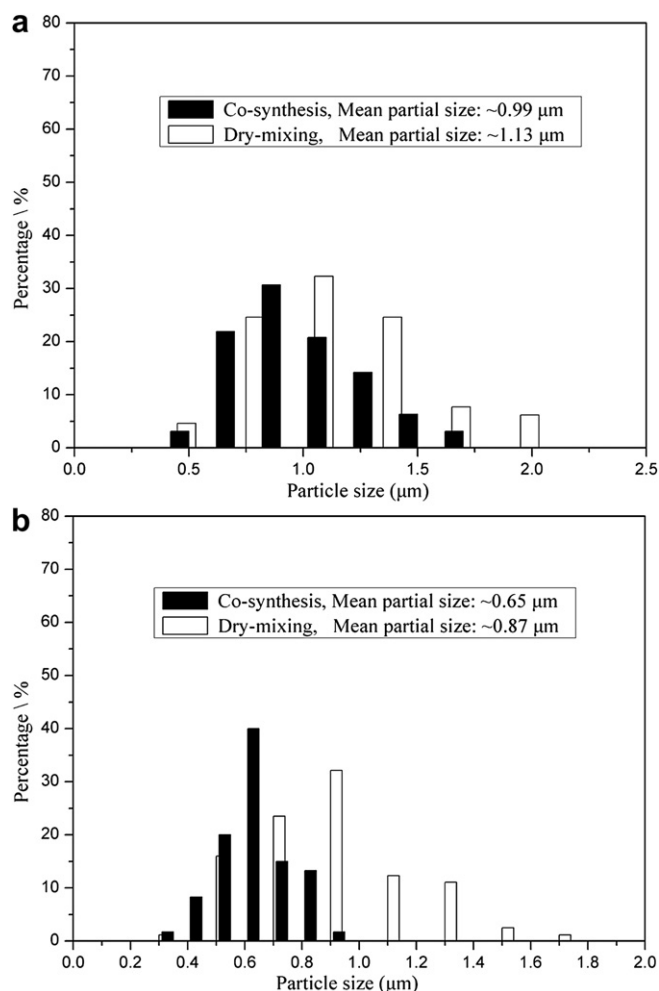


Fig. 3. The grain size distribution of SSF (a) and SDC (b) in two samples.

circuit voltage conditions at 600 °C, cell A with co-synthesis cathode and cell B with dry-mixing cathode. In order to study different processes that happen at electrode, it is significant that to explain the different semicircles involved. At high frequencies the impedance arcs are attributed to oxygen ion transfer across electrode/electrolyte boundary into electrolyte; the arcs at low frequencies are assigned to oxygen ion diffusion through the electrode layer and the charge transfer reaction at cathode surface [25]. For clarity, only the contribution associated with polarization resistance ( $R_p$ ) were shown, while the  $R_b$  corresponding to bulk resistance was omitted. It is easy to find that, comparing to cell A, the cell B semicircle at low frequencies is larger and provides a greater contribution to the  $R_p$  of electrode. This result confirms that oxygen ions are more easily generated and transported in the electrode of cell A, probably due to high surface activity and conductivity in this electrode which is more favorable to the production and transportation of oxygen ion. In  $\text{Gd}_{0.2}\text{Sr}_{0.8}\text{FeO}_{3-\delta}$ - $\text{Ce}_{0.8}\text{Gd}_{0.2}\text{O}_{3-\delta}$  oxygen permeation membrane [24], the sample derived from one-step method exhibited high oxide permeation performance, which demonstrated our deduction to a certain extent.

The ASRs of two kind electrodes in temperature range of 500–700 °C are shown in Fig. 5(b). As can be seen, an obvious drop of ASR is observed for two cells with increasing temperature. More importantly, ASR of cell A is invariably lower than that of cell B at

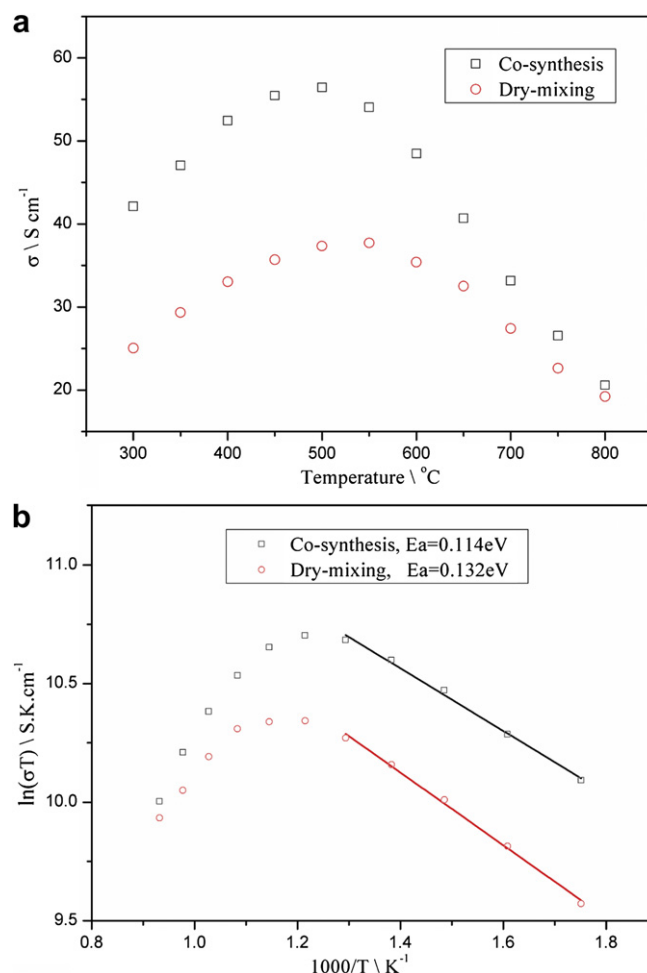
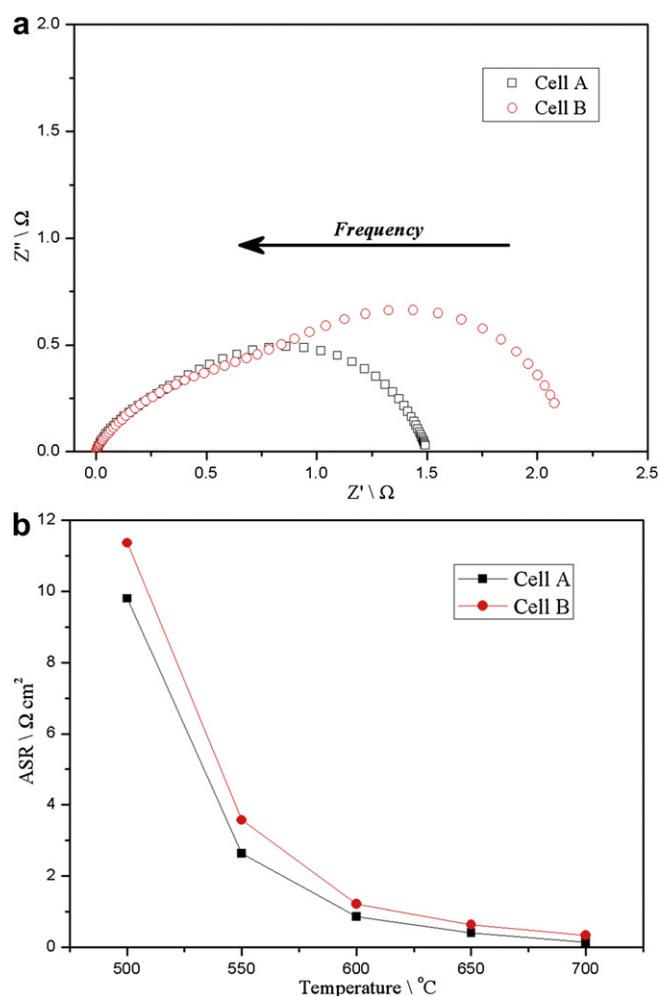


Fig. 4. Temperature dependence of conductivity (a) and corresponding Arrhenius plots (b) of different SSF–SDC samples.

same temperature which can be interpreted by above discussion. The ASRs of cell A are 0.14, 0.40, 0.87, 2.6, 9.8  $\Omega \text{ cm}^2$  at 700, 650, 600, 550, 500 °C, respectively. These values are comparable with those reported for other cobalt-free cathodes [26,27].

### 3.5. Cathode evaluation

The SSF–SDC cathode derived from new synthesis method showed high electrical conductivities and good electrochemical properties. So a single cell based on the corresponding cathode was assembled and tested to evaluate cathode performance.  $I$ – $V$  and  $I$ – $P$  plots of the single SOFC were displayed in Fig. 6(a). The open circuit voltage values and the peak power densities respectively are 0.78 V and 523  $\text{mW cm}^{-2}$  at 700 °C, 0.81 V and 351  $\text{mW cm}^{-2}$  at 650 °C, 0.85 V and 249  $\text{mW cm}^{-2}$  at 600 °C. The open circuit voltages are lower than those of the cells with other electrolytes at same temperature, due to the reduction of  $\text{Ce}^{4+}$  to  $\text{Ce}^{3+}$  in doped ceria which causes the introduction of electronic conductivity [28]. Nevertheless, comparing with other SDC cells they are normal and acceptable values [29]. The fuel-cell performance might be further improved by optimizing the cell structure, such as reducing current leaking using YSZ thin layer. The polarization behavior of cathode on the single SOFC was described in Fig. 6(b). The polarization resistance decreased from 0.335 to 0.074  $\Omega \text{ cm}^2$  with increasing temperature from 600 to 700 °C, comparable with other cell with cobalt-free cathode [30,31].



**Fig. 5.** EIS of symmetric cells with different cathode at 600  $^{\circ}\text{C}$ , cell A corresponding to co-synthesis cathode; cell B corresponding to dry-mixing cathode. (a) The ASR comparison from 400 to 800  $^{\circ}\text{C}$ . (b).

After testing, the tri-layer cell structure is presented by SEM technology. As shown in Fig. 7, there are two porous electrodes, anode and cathode, well adhered on both side of dense SDC electrolyte, suggesting a good thermal matching between parts. The thickness of the electrolyte is about 20  $\mu\text{m}$  and that of the cathode about 40  $\mu\text{m}$ .

The thermal expansion curve is shown in Fig. 8 and the TEC achieves  $17.2 \times 10^{-6} \text{ K}^{-1}$  in temperature range of 50–800  $^{\circ}\text{C}$ . It is obvious that the TEC of SSF is much close to SDC ( $12.4 \times 10^{-6} \text{ K}^{-1}$  [32]) than that of Co-containing cathode, such as  $\text{SmBaCo}_2\text{O}_{5+\delta}$  ( $24.1 \times 10^{-6} \text{ K}^{-1}$ ) [33],  $\text{Sm}_{0.5}\text{Sr}_{0.5}\text{CoO}_{3-\delta}$  ( $22.3 \times 10^{-6} \text{ K}^{-1}$ ) [34]. The close TECs ensure the good matching between SSF cathode and SDC electrolyte and then minimize the occurrence of delamination or crack in cathode/electrolyte interface.

To investigate the thermal cycle performance of Fe-based cathode and Co-based cathode, two symmetrical cells with SSF–SDC and  $\text{Sm}_{0.5}\text{Sr}_{0.5}\text{CoO}_{3-\delta}$ – $\text{Ce}_{0.8}\text{Sm}_{0.2}\text{O}_{1.9}$  (SSC–SDC) cathode were applied to thermal cycle test and the temperature was periodically varied between 200 and 700  $^{\circ}\text{C}$ . As shown in Fig. 9, the initial polarization resistance ( $R_o$ ) of SSC is low than that of SSF and the polarization resistances ( $R_p$ ) of SSC and SSF increase with the increasing of cycle time. The rising of  $R_p$  was represent by the change rate of  $R_p$  ( $\eta$ ):  $\eta = (R_p - R_o)/R_p$ .  $\eta = 36\%$  for SSC and  $\eta = 16\%$

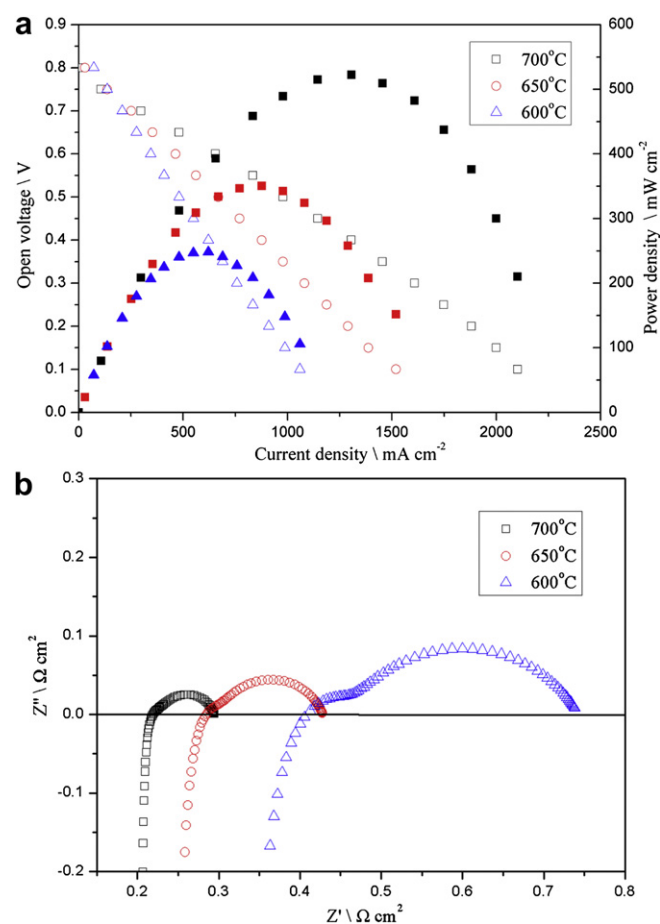


**Fig. 6.** Cell performance (a) and EIS (b) of a single cell with SSF–SDC composite cathode obtaining by co-synthesis method at 600–700  $^{\circ}\text{C}$ .

for SSF can be obtained after 40 cycles, suggesting that SSC have a more quick performance degeneration. This phenomenon can be explained from the view of TEC. In course of heating or cooling, the stress was yielded at the cathode/electrolyte interface, resulting in the increasing of  $R_p$ . The TEC of SSC is larger than that of SSF and thereby  $\eta$  is higher.

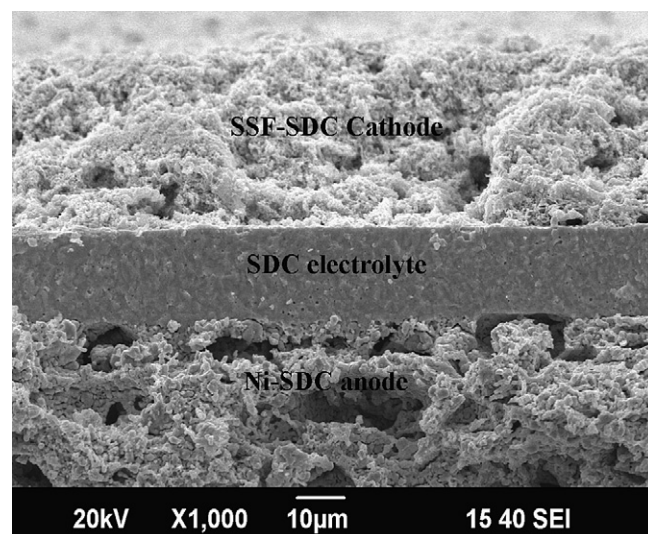


**Fig. 7.** Cross-section SEM images of a single cell after testing.

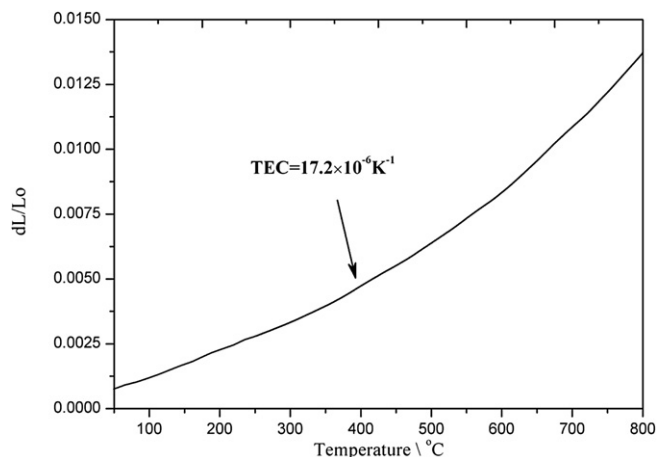


Fig. 8. Thermal expansion ( $dL/L_0$ ) curve of SSF in the temperature range of 300–800 °C in air.

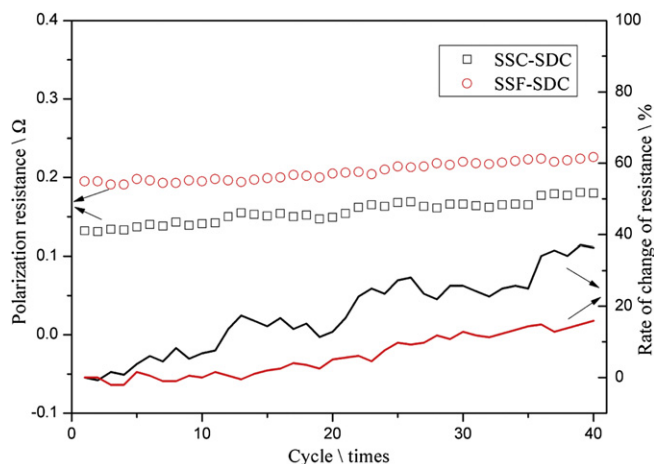


Fig. 9. The comparison of thermal cycling performance of SSF–SDC and SSC–SDC as the cathode performed in the temperature range of 200–700 °C.

#### 4. Conclusions

In this paper, co-synthesis method was used to synthesis SSF–SDC cathode. Comparing to traditional dry-mixing method, the samples from co-synthesis method showed identical phase structure, superior microstructure, high electrical conductivity and good catalytic activity. As expected, a homogeneous two-phase distribution and small grain size in sample derived from co-synthesis method promoted electrochemical properties of SSF–SDC. The cobalt-free SSF–SDC cathode was developed as cathode of SOFC with SDC electrolyte. The polarization resistances

of the cell were comparable to those observed for other cobalt-free cathodes. The thermal cycle tests suggested that SSF–SDC cathode owned a better cycling stability than SSC–SDC. A preferable properties and simple preparation process are meaningful for practical application as SOFC cathode.

#### Acknowledgment

This work is kindly supported by the National Natural Science Foundation of China (Grant No: 21076204) and the Ministry of Science and Technology of China (Grant No: 2012CB215403).

#### References

- [1] J. Molenda, K. Świerczek, W. Zajac, J. Power Sources 173 (2007) 657–670.
- [2] N. Ai, Z. Lü, K. Chen, X. Huang, Y. Liu, R. Wang, W. Su, J. Membr. Sci. 286 (2006) 255–259.
- [3] C. Lu, S. An, W.L. Worrell, J.M. Vohs, R.J. Gorte, Solid State Ionics 175 (2004) 47–50.
- [4] N. Benoved, O. Kesler, J. Power Sources 193 (2009) 454–461.
- [5] A.B. Stambouli, E. Traversa, Renew. Sust. Energy Rev. 6 (2002) 433–455.
- [6] J. Fleig, Annu. Rev. Mater. Res. 33 (2003) 361.
- [7] K. Zhang, L. Ge, R. Ran, Z. Shao, S. Liu, Acta Mater. 56 (2008) 4876–4889.
- [8] J.-H. Kim, A. Manthiram, J. Electrochem. Soc. 155 (2008) B385–B390.
- [9] W. Zhou, R. Ran, Z. Shao, W. Jin, N. Xu, J. Power Sources 182 (2008) 24.
- [10] Y. Takeda, K. Kanno, T. Takada, O. Yamamoto, M. Takano, N. Nakayama, Y. Bando, J. Solid State Chem. 63 (1986) 237.
- [11] J. Mizusaki, M. Okayasu, S. Yamauchi, K. Fueki, J. Solid State Chem. 99 (1992) 166.
- [12] Y. Niu, W. Zhou, J. Sunarso, L. Ge, Z. Zhu, Z. Shao, J. Mater. Chem. 20 (2010) 9619.
- [13] J. Chen, S. Wang, T. Wen, J. Li, J. Alloys Compd. 487 (2009) 379.
- [14] C.R. Dyck, Z.B. Yu, V.D. Krstic, Solid State Ionics 171 (2004) 17.
- [15] C.-L. Chang, C.-S. Hsu, B.-H. Hwang, J. Power Sources 179 (2008) 734–738.
- [16] Y. Chen, D. Chen, R. Ran, H.J. Park, C. Kwak, S.J. Ahn, K.S. Moon, Z. Shao, Electrochem. Commun. 14 (2012) 36–38.
- [17] H. Gu, H. Chen, L. Gao, L. Guo, Electrochim. Acta 54 (2009) 7094–7098.
- [18] M. Juhl, S. Primdahl, C. Manon, M. Mogensen, J. Power Sources 61 (1996) 173–181.
- [19] J. Højberg, M. Søgaard, Electrochim. Solid-State Lett. 14 (2011) B77–B79.
- [20] Z. Zhu, W. Sun, L. Yan, W.F. Liu, W. Liu, Int. J. Hydrogen Energy 36 (2011) 6337–6342.
- [21] Q. Li, X. Zhu, W. Yang, J. Membr. Sci. 325 (2008) 12.
- [22] L. Kindermann, D. Das, H. Nickel, K. Hilpert, Solid State Ionics 89 (1996) 215–220.
- [23] G.C. Kostoglou, G. Tsiniarakis, C. Ftikos, Solid State Ionics 135 (2000) 529–535.
- [24] X. Zhu, H. Wang, W. Yang, J. Membr. Sci. 309 (2008) 120–127.
- [25] N. Ortiz-Vitoriano, I. Ruiz de Larramendi, I. Gil de Muro, A. Larrañaga, J.I. Ruiz de Larramendi, T. Rojo, J. Mater. Chem. 21 (2011) 9682–9691.
- [26] Q. Zhou, L. Zhang, T. He, Electrochem. Commun. 12 (2010) 285–287.
- [27] G. Zhu, X. Fang, C. Xia, X. Liu, Ceram. Int. 31 (2005) 115–119.
- [28] A.J. Jacobson, Chem. Mater. 22 (2010) 662.
- [29] B. Lin, J. Chen, Y. Ling, X. Zhang, Y. Jiang, L. Zhao, X. Liu, G. Meng, J. Power Sources 195 (2010) 1624–1629.
- [30] Y. Ling, L. Zhao, B. Lin, Y. Dong, X. Zhang, G. Meng, X. Liu, Int. J. Hydrogen Energy 35 (2010) 6905–6910.
- [31] B. Wei, Z. Lü, X. Huang, M. Liu, N. Li, W. Su, J. Power Sources 176 (2008) 1–8.
- [32] Y. Zheng, H. Gu, H. Chen, L. Gao, X. Zhu, L. Guo, Mater. Res. Bull. 44 (2009) 775–779.
- [33] Z. Zhu, Z. Tao, L. Bi, W. Liu, Mater. Res. Bull. 45 (2011) 1771–1774.
- [34] S.W. Baek, J.H. Kim, J. Bae, Solid State Ionics 179 (2008) 1570–1574.